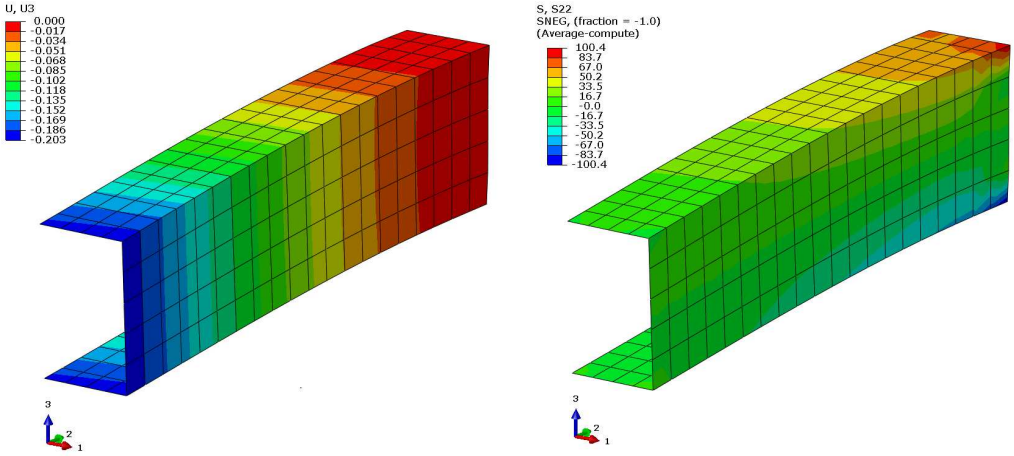

Figure 6.38. Displacement and longitudinal stress with the beam loaded in the shear center.

Figure 6.38 presents the results for this new condition; now the beam exhibits the typical bending behavior, but the values of the longitudinal stress are in agreement with the theoretical results only in the middle, while at the clamp they still present, although in a less marked form, a variation along the transversal direction, in this case certainly attributable to the presence of the constraint.

We have already said that some pre/post-processors are able to manage the beam sections, calculating the inertial characteristics starting from the geometric dimensions; many go further and, at least for some types of section, are able to determine the shear center. It is necessary, however, to pay much attention to what the calculation code then does, i.e. it is necessary to verify whether or not the section is translated in the shear center or if it is left on the centroidal axis; in fact, as we have seen, the results can change a lot, for some sections, in the two cases.

Finally we underline that in carpentry constructions the beams are connected with each other (by riveting, bolting or welding) in such a way that it is impossible to ensure that shear loads are applied in the torsion centers of the beams themselves. Therefore generally this type of beams will be subject to the phenomenon we have seen; a beam element schematization could filter this effect making it necessary an accurate results interpretation phase, downstream of the finite element calculation.

6.3.3.6 Large-curvature beam

In the last example of this paragraph we want to calculate the beam of figure 6.39, loaded at one end with a force F = 300000 N and clamped at the other. The most stressed section turns out to be the one that is found to the greater distance from the line of application of the force F; in this section are present an axial force equal to 300 kN and a bending moment equal to 120000 kNmm.

If we suppose to consider the beam as straight (i.e., as if the height h of the section were negligible with respect to the radius r_0 of curvature of the centroidal fiber), the maximum stress in the most loaded section holds:

$$\sigma = \pm \frac{F \cdot r_0}{I_{yy}} \cdot \frac{h}{2} + \frac{F}{A}$$

Being $I_{yy} = 60000000$ mm^4 and $A = 18000$ mm^2, at the intrados and extrados of the beam the following stress values are obtained:

$$\sigma_i = \frac{F \cdot r_0}{I_{yy}} \cdot \frac{h}{2} + \frac{F}{A} = 216.7 \text{ MPa} \qquad \sigma_e = -\frac{F \cdot r_0}{I_{yy}} \cdot \frac{h}{2} + \frac{F}{A} = 183.3 \text{ MPa}$$

However, the value of h is comparable with that of r_0 and therefore it is not permissible to consider the beam as if it were straight. One of the effects that occurs in beams with large curvature undergoing bending is the displacement of the neutral axis: in other words, the fibers with zero stress no longer lie on the centroidal axis; this results in a different distribution of stresses within the section, which alters the minimum and maximum values.

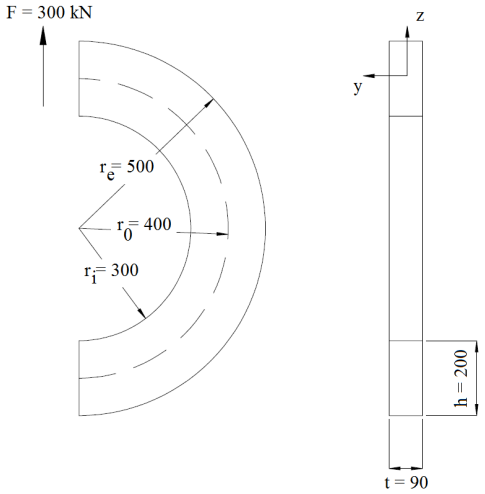

Figure 6.39. Large curvature beam

In the most stressed section, the value of the stress in the tangential direction that is obtained from the second-order theory valid for large-curvature beams is given by the following relationship:

$$\sigma = \frac{F \cdot r_0}{A \cdot (r_0 - r_n)} \cdot \frac{r_n - r}{r} + \frac{F}{A}$$

where r_n is the radius that locates the neutral axis with respect to the center of curvature and r is the generic radial coordinate at which the stress is evaluated. Being:

$$r_n = \frac{r_e - r_i}{\ln \frac{r_e}{r_i}} = 391.5 \text{ mm}$$

and placing $r = r_i = 300$ mm we obtain the value of the tangential stress at the intrados of the beam: $= \sigma$ 257 MPa.

Instead, placing $r = r_e = 500$ mm we obtain the value of the stress at the extrados of the beam: $= \sigma$ -154 MPa.

The remarkable difference between the two cases (straight beam and curved beam) is self-explanatory. Wanting to perform a numerical calculation, we could naively think that the implementation of a beam element model may be sufficient to capture this important effect: nothing could be more wrong. And dangerous.

We then build the beam element model, in this case taking advantage of the software's ability to handle a rectangular section. Figure 6.40 shows such a model, while in figure 6.41 we illustrate the results obtained.

As it can be seen, the agreement with the results obtained with the first-order theory is perfect, as was to be expected. The fact of having exploited the capabilities of the computational code and the pre/post-processor to handle the sections for beam elements does not allow to cross the intrinsic limit of this type of element.

We observe then the displacement that the force application undergoes in the direction of the force itself: u_2 = 2.49 mm; this information will be useful for the comparison with the next model.

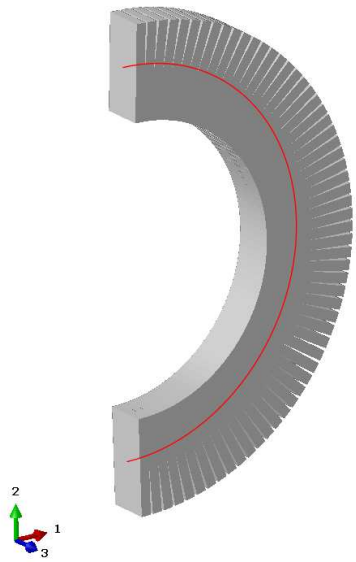

Figure 6.40. Beam element model for the large curvature beam; elements are shown in red. The section is centered at the center of gravity.

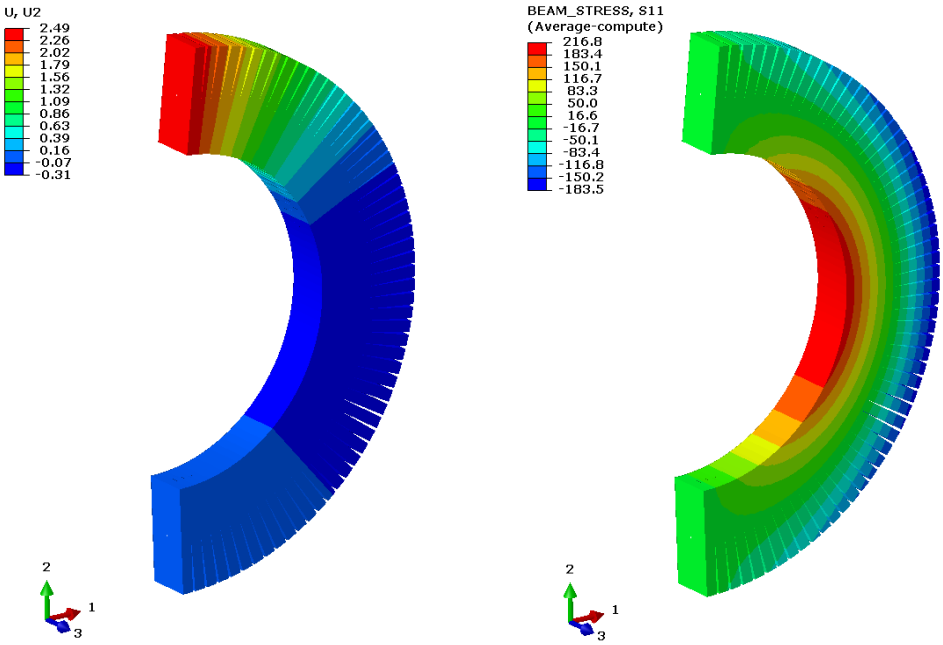

Figure 6.41. Displacement in the vertical direction and stress along the (curvilinear) axis of the beam.

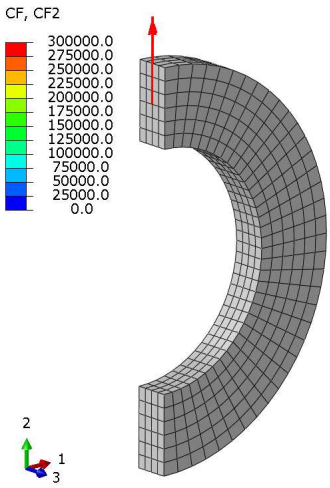

Figure 6.42. Brick element model for the large curvature beam.

We construct therefore, more realistically, a model of the beam using brick elements (figure 6.42) because of the elevated thickness (even if plane strain elements could be employed) and we execute on it the calculation. Figure 6.43 shows the contour of the displacement in the vertical direction and of the circumferential stress in a cylindrical reference system suitably constructed in the center of the circular crown. Comparing these data with the manual calculation performed in accordance with second-order theory, we conclude that the brick-element model is adequate to capture the effect of the neutral axis shift.

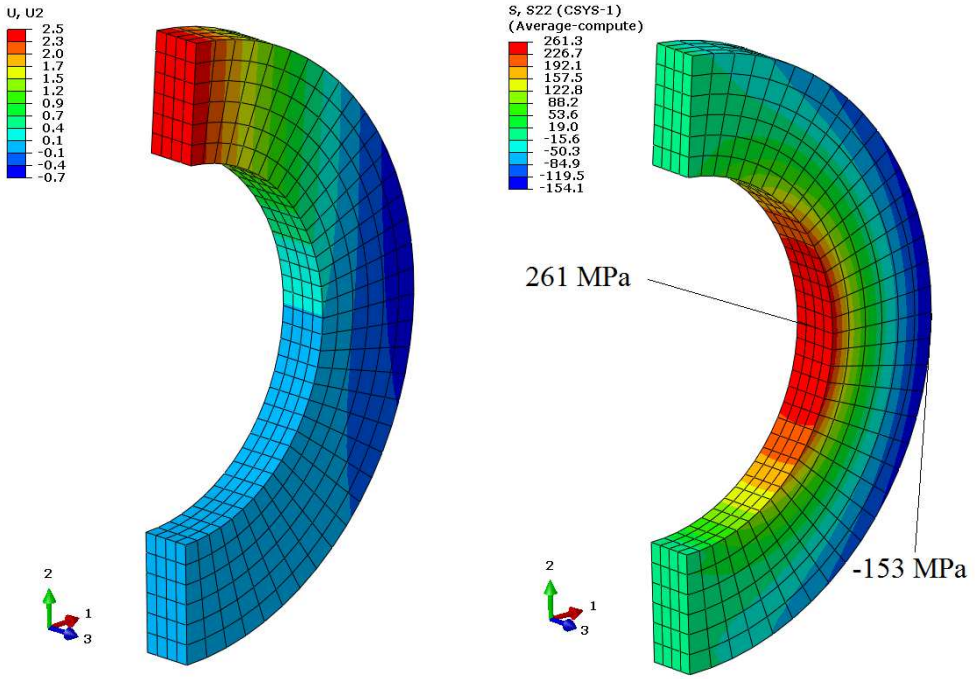

Figure 6.43. Displacement in the vertical direction (left) and stress along the circumferential direction of a cylindrical reference system (right).

A further consideration concerns the displacement of the force application point, which in this case is $u_z = 2.5$ mm.

We can therefore state that, while the error on displacements with the beam element model is practically null, indicating how the beam stiffness provided by the beam element model is very close to the real value, the error on the maximum stress is 19%.

At this point, some observations are necessary. While through the shell and brick element models it is possible to take into account the real constraint, load and geometric conditions, allowing to capture effects such as the torsion, which we could define "parasitic", illustrated in the example of the C-section beam, or the displacement of the neutral axis, highlighted with the last example, with beam elements this is not possible due to their mathematical formulation: as already mentioned (see Chapter 1) they are one-dimensional elements that lie along the centroidal axis of the beam they must simulate; moreover, except for particular implementations, they are based on the theory valid for beams with a rectilinear axis. An increase of the mesh density, which in other circumstances would bring closer to the "exact" result, in this case would serve no purpose.

All this does not mean that beam elements should be banned from numerical analyses of structures, quite the contrary. Their usefulness is notable and beyond discussion in numerous cases, such as in modal analyses, where the values of the stiffnesses and masses are fundamental, while local effects are less important, as we saw in Chapter 4. Here we only wanted to draw attention to the prudence that must be adopted when attempting to simplify a calculation by reducing the structure to be analyzed to a series of "equivalent beams": many important effects that influence the real states of deformation and stress may be lost, completely falsifying the results of the analysis.

6.3.3.7 The skinning technique

Although the choice of the brick element for the large-curvature beam is the correct one, this type of element also has inherent errors. Let's see which ones.

In figure 6.44 we illustrate the three principal stresses for the element extracted at the intrados of the large curvature beam in the most stressed section. The representation is by means of arrows indicating the intensity and direction of the quantities under examination (in the Gauss points; this is the reason why the value in the figure at the top right is less than that shown in figure 6.43 - see § 3.9.5).

As it can be observed, and as we know, the three main stresses are orthogonal to each other. However, we expect that, at least on the "free" face of the considered element (i.e. the one in contact with the air), the intermediate principal stress is zero, because on the surface of a solid not submitted to pressure, the stress state must be plane for equilibrium. But this is not the case. And this is an inherent "error" in FEM: the indefinite equilibrium equations (see Appendix B) are not always met. However, it must be said that the equilibrium equations of the forces at the nodes connecting the elements are instead respected.

This error tends to decrease the finer the mesh is; in fact, if we double the number of elements in the radial direction, we obtain the results of figure 6.45, where the value of the intermediate principal stress has almost halved.

A method to overcome this drawback without necessarily having to refine the mesh (which would not be necessary, given the remarkable agreement with the theoretical results obtained with the base model) is to resort to skinning, i.e. the covering of the solid with membrane elements (see § 1.9), very thin in order not to alter the stiffness